

Analysis on the evolution of $\sigma_8(z)$ from Linear Nash-Greene fluctuations

Abraão J. S. Capistrano,^{a,d1} Luís A. Cabral,^{b,d} José A. P. F. Marão^c Carlos H. Coimbra-Araújo^{a,d}

^aUniversidade Federal do Paraná, 85950-000, Palotina-PR, Brazil

^bUniversidade Federal do Tocantins, 77824-838, Araguaína-TO, Brazil

^cUniversidade Federal do Maranhão, 65085-580, São Luís-MA, Brazil

^dApplied Physics Program, UNILA, 85867-670, Foz do Iguassu-PR, Brazil.

E-mail: abecapistrano@gmail.com, cabral@uft.edu.br, jose.marao@ufma.br, carlos.coimbra@ufpr.br

Abstract. From the linear Nash-Greene fluctuations of background metric, we present the perturbation equations in an embedded four space-time. In the context of a five-dimensional bulk, we show that the perturbations are only propagated by the gravitational tensorial field equation. In Newtonian conformal gauge, we study the matter density evolution in sub-horizon regime and on how such scale may be affected by the extrinsic curvature. We apply a joint likelihood analysis to the data with the Markov Chain Monte Carlo (MCMC) method for cosmological parameter estimation using a pack of recent datasets as the Pantheon Supernovae type Ia, the Baryon Acoustic Oscillations (BAO) from DR12 galaxy sample and Dark Energy Survey (DES) Y1. The constrained parameters are tested in the cosmography analysis on the evolution of Hubble function $H(z)$ and the deceleration parameter $q(z)$, as well as on the evolution of the growth rate $f\sigma_8(z)$ of the “extended Gold 2018” growth-rate dataset with 25 datapoints. Moreover, we obtain an alleviation of the σ tension in the contours between $(\sigma_8-\Omega_m)$ of the observations from Cosmic Microwave Background (CMB) and large scale structure (LSS) probes.

¹Corresponding author.

Contents

1	Introduction	1
2	The induced embedded equations	3
2.1	The Einstein-Hilbert principle for a five dimensional bulk	3
2.2	The integrability of the embedding and the bulk metric	4
2.2.1	The dynamical embedding: the Nash flow	5
2.2.2	Integrability conditions and induced equations	7
3	Background FLRW metric	8
3.1	Non perturbed field equation in an embedded space-time	9
3.2	Hydrodynamical equations	9
4	Transformations and gauge variables	10
5	Scalar perturbations in Newtonian gauge	13
5.1	Perturbed gravitational equations	13
5.2	Hydrodynamical gravitational perturbed equations	14
6	Matter density evolution under subhorizon regime	15
7	Analysis on evolution of $f\sigma_8(z)$ and σ_8-tensions	16
8	Remarks	21
9	Acknowledgements	23

1 Introduction

The Occam’s razor is one of the cornerstone philosophical principles in science that states that the simplest solution of a problem should be adopted in detriment of the complex ones. In this realization, the Λ CDM model has been the simplest and successful solution to deal with the accelerated expansion of the universe as corroborated for several independent observations in the last two decades [1–10, 12]. Despite its success, the Λ CDM model has important drawbacks that must be taken into account. For instance, the main components of Λ CDM model lack a fundamental explanation about the nature of the cosmological constant Λ and also the (Cold) Dark Matter (CDM) problem [13–19].

In this paper, we focus on studying the σ -tension in the σ_8 -contours revealed by the mismatch of the data inferred from Cosmic Microwave Background (CMB) radiation probe and the large scale structure (LSS) observations, considering the concordance Λ CDM model as a background. The σ_8 is the r.m.s amplitude of matter density at a scale of a radius $R \sim 8h\text{Mpc}^{-1}$ within a enclosed mass of a sphere [20]. The main problem apparently resides in the fuzzy origin of such mismatch, which could be a result of systematics or due to deviations of gravity. The situation still resists in both early and late universe landscapes even if one does not consider the Planck CMB data [21] and evidences that similar discrepancies may also occur in the matter distributions around $2\text{-}\sigma$ [12, 22–24]. In particular, to avoid

a biased dependence of σ_8 , the quantity $f\sigma_8(z)$ is a good model-independent discriminator for mapping the growth rate of matter. This alleged discrepancy opens an interesting arena for testing gravitational models, once the possibility to alleviate it may come from modified gravity or extensions [25–31].

In the context that gravity may be modified departed from Einstein gravity or other fundamental principle, we explore the embedding of geometries (or hypersurfaces) to elaborate a model independent based on seminal works on the subject [32–34] in order to tackle the aforementioned σ_8 -issue in the problem of explanation of the accelerated expansion of the universe. In hindsight, the seminal problem of embedding theories lies in the hierarchy problem of fundamental interactions. The possibility that gravity may access extra-dimensions is taken as a principle for solving the huge ratio of the Planck masses (M_{Pl}) to the electroweak energy scale M_{EW} in such $M_{Pl}/M_{EW} \sim 10^{16}$. This option has been explored more vigorously in the last two decades as a solution to the dark energy paradigm. Most of these models have been Kaluza-Klein or/and string inspired, such as, for instance, the works of the Arkani-Hamed, Dvali and Dimopolous (ADD) model [35], the Randall-Sundrum model [36, 37] and the Dvali-Gabadadze-Porrati model (DPG) [38]. Differently from these models with specific conditions, and apart from the braneworld standards and variants, we have explored the embedding as a fundamental guidance for elaboration of a gravitational physical model. Until then, several authors explored the embedding of geometries and its physical consequences as a mathematical structure to apply to gravitational problems [32–34, 39–52].

The plan of the paper is organized in sections. In the second section, we revise the embedding of geometries and how it may be used to construct a physical framework. In this context, the Nash-Greene theorem is discussed. The third and fourth sections verse on the background Friedmann–Lemaître–Robertson–Walker (FLRW) metric, transformations and gauge variables also involving the extrinsic curvature, respectively. The fifth section shows the resulting conformal Newtonian gauge equations. In the sixth section, we show the contrast matter density $\delta_m(a)$ as a result of the Nash fluctuations and an effective Newtonian constant G_{eff} is also determined that carries a signature of the extrinsic curvature. In the seventh section, using a MCMC sampler relying on the Code for bayesian analysis (Cobaya)¹ [53, 54] to constrain the parameters, we make a joint analysis of data taking into account the evolution of background parameter $H(z)$ and Ω_m distributions from SNIa Pantheon data [55], clustering and weak lensing from DES Y1 [56], the DR12 “consensus” galaxy sample [57] to compute growth data, $H(z)$ and BAO. The MCMC chains were analyzed by using GetDist² [58]. By the constraints of the parameters, we apply a cosmography test on the models based on the evolution of $H(z)$ and the deceleration parameter $q(z)$ and compare our models, also mimicking Λ CDM model, in analysing the curves from $f\sigma_8(z)$ measurements by using the “extended Gold 2018” compilation of the data points of SDSS [59–61], 6dFGS [62], IRAS [63, 64], 2MASS [63, 65], 2dFGRS [66], GAMA [67], BOSS[68], WiggleZ [69], Vipers [70], FastSound [71], BOSS Q [72] and additional points from the 2018 SDSS-IV [27, 73–75]. In the final section, we present our remarks and prospects.

It is noteworthy to point out that we adopt the Landau time-like convention (− − − +) for the signature of the four dimensional embedded metric and speed of light $c = 1$. Concerning notation, capital Latin indices run from 1 to 5. Small case Latin indices refer to the only one extra dimension considered. All Greek indices refer to the embedded space-time counting from

¹<https://github.com/CobayaSampler/cobaya>

²<https://github.com/cmbant/getdist>

1 to 4. Hereon we indicate the non-perturbed (background) quantities by the upper-script symbol “0”.

2 The induced embedded equations

In the following subsections, we present our theoretical framework. First, the embedding of geometries is presented that creates a mathematical background landscape for a physical model to be developed. Secondly, by pursuing this intent, the induced field equations of the embedded space-time are presented that result from the integrability of the embedding given by Nash-Greene theorem to arise a viable physical framework.

2.1 The Einstein-Hilbert principle for a five dimensional bulk

Although embeddings can be made in an arbitrary number of dimensions (see [32–34, 42, 43, 46–49, 51, 52]), the current alternative models of gravitation are normally stated in five dimensions at most. Then, we start with a model defined by a gravitational action functional in the presence of confined matter field on a four-dimensional embedded space-time embedded in a five-dimensional larger space that has the form

$$S = -\frac{1}{2\kappa_5^2} \int \sqrt{|\mathcal{G}|} {}^5\mathcal{R} d^5x - \int \sqrt{|\mathcal{G}|} \mathcal{L}_m^* d^5x, \quad (2.1)$$

where κ_5^2 is a fundamental energy scale on the embedded space, ${}^5\mathcal{R}$ denotes the five dimensional Ricci scalar of the bulk and \mathcal{L}_m^* denotes the confined matter Lagrangian in such the matter energy momentum tensor fulfills a finite hypervolume with constant radius l along the fifth-dimension. Thus, the variation of Einstein-Hilbert action in Eq.(2.1) with respect to the bulk metric \mathcal{G}_{AB} leads to the Einstein equations

$${}^5\mathcal{R}_{AB} - \frac{1}{2} {}^5\mathcal{R} \mathcal{G}_{AB} = \alpha^* \mathcal{T}_{AB}, \quad (2.2)$$

where α^* is the energy scale parameter and \mathcal{T}_{AB} is the energy-momentum tensor for the bulk [32–34, 43]. In accordance with the Nash-Greene theorem [76, 77], it verses on orthogonal perturbations of the metric which induce the appearance of the extrinsic curvature in that direction. To our purposes, we are restricted to the four-dimensionality of the space-time embedded in a five dimensional bulk space following the confinement hypothesis [78, 79] and such dimensionality will suffice based on experimentally high-energy tests [80].

This model can be regarded as a four-dimensional hypersurface dynamically evolving in a five-dimensional bulk with constant curvature whose related Riemann tensor is

$${}^5\mathcal{R}_{ABCD} = K_* (\mathcal{G}_{AC}\mathcal{G}_{BD} - \mathcal{G}_{AD}\mathcal{G}_{BC}), \quad A...D = 1...5,$$

where \mathcal{G}_{AB} denotes the bulk metric components in arbitrary coordinates and the constant curvature K_* is either zero (flat bulk) or it can have positive (deSitter) or negative (anti-deSitter) constant curvatures.

In accordance with recent observations [12], with a very small value of the cosmological constant Λ , we do not consider any dynamical contribution of such quantity. Then, we chose $K_* = 0$, although our results also hold for any other choice of K_* . The bulk geometry is actually defined by the Einstein-Hilbert principle in Eq.(2.1), which leads to Einstein’s equations as shown in Eq.(2.2). The confinement condition implies that $K_* = \Lambda_*/6 = 0$ and

the confined components of \mathcal{T}_{AB} are proportional to the energy-momentum tensor like that of general Relativity (GR): $\alpha_* T_{\mu\nu} = 8\pi G_N T_{\mu\nu}$, where G_N is the bare gravitational Newtonian constant. On the other hand, since only gravity propagates in the bulk we have $T_{\mu a} = 0$ and $T_{ab} = 0$. In this sense, it is possible to search a more general physical theory based on the geometries of embedding. Although it is not explicitly showed here, depending on the type of the embedding (e.g., local or global, isometric, analytic or differentiable, etc.), brane-world models may be an example of this framework [33]. Another important aspect of the original Nash embedding is that it is applied to a flat D -dimensional Euclidean space. It was explored in a work by J. Rosen [81] with an analysis on pseudo-Euclidean spaces. Its generalization to pseudo-Riemannian manifolds to non-positive signatures results that the embedding of the space-times may need a larger number of dimensions was made only two decades later by Greene [77]. Hereon, we simply call the Nash-Greene theorem.

In a nutshell, the smoothness of the embedding is the cornerstone of the Nash-Greene theorem, once this embedding results from a differentiable mapping of functions of the manifolds. On the other hand, it is not capable of telling us about the physical dynamic equations or evolution of the gravitational field by its own. Thus, a natural choice for the bulk is that its metric satisfies the Einstein-Hilbert principle. By design, it represents the variation of the Ricci scalar and the related curvature must be “smoother” as possible [42]. It warrants that the embedded geometry and their deformations will be differentiable too.

2.2 The integrability of the embedding and the bulk metric

Let a Riemannian manifold V_4 be endowed with a non-perturbed metric $^{(0)}g_{\mu\nu}$ being locally and isometrically embedded in a five-dimensional Riemannian space V_5 . Given a differentiable and regular map $\mathcal{X} : V_4 \rightarrow V_5$, one imposes the embedding equations

$$\mathcal{X}_{,\alpha}^A \mathcal{X}_{,\beta}^B \mathcal{G}_{AB} = g_{\alpha\beta}^{(0)} , \quad (2.3)$$

$$\mathcal{X}_{,\alpha}^A {}^0\eta_a^B \mathcal{G}_{AB} = 0 , \quad (2.4)$$

$${}^0\eta_a^A {}^0\eta_b^B \mathcal{G}_{AB} = 1 , \quad (2.5)$$

where we have denoted \mathcal{X}^A the non-perturbed embedding coordinate, \mathcal{G}_{AB} the metric components of V_5 in arbitrary coordinates, and ${}^0\eta$ denotes the non-perturbed unit vector field orthogonal to V_4 . This mechanism avoids possible coordinate gauges that may drive to false perturbations. The colons denote ordinary derivatives.

The meaning of those former set of equations is that Eq.(2.3) represents the isometry condition between the bulk and the embedded space-time. The orthogonality between the embedding coordinates \mathcal{X} and ${}^0\eta$ is represented in Eq.(2.4). Moreover, Eq.(2.5) denotes the set of vectors normalization ${}^0\eta$. As a result, the integration of the set of Eqs. (2.3), (2.4) and (2.5) gives the embedding map \mathcal{X} .

The main concern of our work is provide a complement to the Einstein gravity by adding a second curvature, i.e., the extrinsic curvature and to study its implications to a physical theory in five dimensions. As defined in traditional textbooks [82], the extrinsic curvature of the embedded space-time V_4 is the projection of the variation of the vector ${}^0\eta$ onto the tangent plane

$$k_{\mu\nu}^{(0)} = -\mathcal{X}_{,\mu}^A {}^0\eta_{,\nu}^B \mathcal{G}_{AB} = \mathcal{X}_{,\mu\nu}^A {}^0\eta^B \mathcal{G}_{AB} . \quad (2.6)$$

2.2.1 The dynamical embedding: the Nash flow

The dynamical embedding mainly reflects on how the ambient space (the bulk) is related to the embedded space-time. The concept of “pure” Nash deformations are gauge-free since they access the ambient space and are generated by perturbations along the direction orthogonal to V_4 to filter out any coordinate gauges. In five dimensions, this process is simplified and just one deformation parameter suffices to locally deform the embedded background, which can be done by the Lie transport. In a geometrical sense, this is motivated by the notion of the curvature radii of the embedded background. The single curvature radius y_0 is then the smallest of these solutions, corresponding to the direction in which the embedded space-time deviates (is perturbed) more sharply from the tangent plane. The curvature radii of the background must satisfy the homogeneous equation

$$\det(g_{\mu\nu} - y k_{\mu\nu}) = 0 . \quad (2.7)$$

This is a local invariant property of the embedded space-time and does not depend on the chosen Gaussian system [82]. We reinforce the idea that this process occurs in the linkage of the ambient space with the deformations of the space-time and the physical consequences we will analyse after on the induced quantities onto the perturbed embedded (physical) space-time, where the cosmological perturbation theory applies.

As it happens, let a geometric object $\bar{\Omega}$ be constructed in V_4 in any direction ${}^0\eta$ by the Lie transport along the flow for a certain small distance δy . It is worth noting that it is irrelevant if the distance δy is time-like or not, nor it is positive or negative. Then, the Lie transport is given by $\Omega = \bar{\Omega} + \delta y \mathcal{L}_{{}^0\eta} \bar{\Omega}$, where $\mathcal{L}_{{}^0\eta}$ denotes the Lie derivative with respect to the normal vector ${}^0\eta$. In this sense, the Lie transport of the Gaussian coordinates vielbein $\{\mathcal{X}_\mu^A, {}^0\eta_a^A\}$, defined on V_4 , can be written as

$$\mathcal{Z}_{,\mu}^A = \mathcal{X}_{,\mu}^A + \delta y \mathcal{L}_{{}^0\eta} \mathcal{X}_{,\mu}^A = \mathcal{X}_{,\mu}^A + \delta y {}^0\eta_{,\mu}^A , \quad (2.8)$$

$$\eta^A = {}^0\eta^A + \delta y [{}^0\eta, {}^0\eta]^A = {}^0\eta^A . \quad (2.9)$$

Interestingly, from Eq.(2.9), it is straightforward the derivative of ${}^0\eta$ is affected by perturbations in a sense $\eta_{,\mu} \neq {}^0\eta_{,\mu}$.

Concerning perturbations of the embedded space-time V_4 , there is a set of perturbed coordinates \mathcal{Z}^A to satisfy the embedding equations likewise Eqs.(2.3), (2.4) and (2.5), as

$$\mathcal{Z}_{,\mu}^A \mathcal{Z}_{,\nu}^B \mathcal{G}_{AB} = g_{\mu\nu}, \quad \mathcal{Z}_{,\mu}^A \eta^B \mathcal{G}_{AB} = 0, \quad \eta^A \eta^B \mathcal{G}_{AB} = 1 . \quad (2.10)$$

As seen in the non-perturbed case, the perturbed coordinate \mathcal{Z} defines a coordinate chart between the bulk and the embedded space-time.

Replacing Eqs.(2.8) and (2.9) in Eqs.(2.10) and (2.6), for instance, we obtain the fundamentals objects of the new manifold in linear perturbation

$$g_{\mu\nu} = g_{\mu\nu}^{(0)} + \delta g_{\mu\nu} + \dots = g_{\mu\nu}^{(0)} - 2\delta y k_{\mu\nu}^{(0)} + \dots , \quad (2.11)$$

$$k_{\mu\nu} = k_{\mu\nu}^{(0)} + \delta k_{\mu\nu} + \dots = k_{\mu\nu}^{(0)} - 2\delta y {}^0g^{\rho\sigma} k_{\mu\rho}^{(0)} k_{\nu\sigma}^{(0)} + \dots \quad (2.12)$$

Hence, taking the derivative of Eq.(2.11) with respect to deformation parameter y and compare to Eq.(2.12), Nash flow is written as

$$k_{\mu\nu} = -\frac{1}{2} \frac{\partial g_{\mu\nu}}{\partial y} . \quad (2.13)$$

This former expression can be generalized to arbitrary number of dimensions with a set of arbitrary family of orthogonal deformations δy^a .

It is noteworthy to point out that the ADM formulation gives a similar expression later discovered by Choquet-Bruhat and J. York [83]. In a physical context, the interpretation of Eq.(2.13) reinforces the confinement of matter as a consequence of the well established experimental structure of special relativity, particle physics and quantum field theory, using only the observable which interact with the standard gauge fields and their dual properties. It imposes a geometric constraint that it localizes the matter in V_4 [32, 33]. It is important to note that the Nash-Greene fluctuations on the perturbed metric $g_{\mu\nu} = g_{\mu\nu}^{(0)} + \delta g_{\mu\nu} + \delta^2 g_{\mu\nu} + \dots$ are continuously smooth and naturally go on adding small increments $\delta g_{\mu\nu}$ to the background metric. A pictorial view of this process can be seen in Figure (1), where the deformed embedded space-time generates a local bubble of deformation on the original background. Unlike

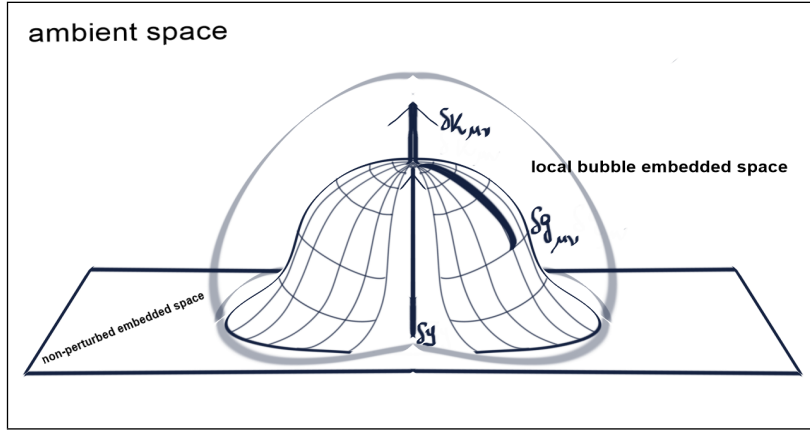


Figure 1. Dynamical embedding in an ambient space. The pictorial “pith helmet” shaped-like emphasizes the embedding bubble formed in the local embedded space-time deformed by the perturbations of the y parameter. The tangent space is orthogonally deformed and the related cosmological perturbations can be studied with a chosen gauge in $\delta g_{\mu\nu}$.

those of processes of rigid embedding models [36, 37], where the deformation parameter y is commonly inserted in the line element to obtain cosmological perturbations with additional assumptions; in dynamical embeddings, the orthogonal deformations parameter y accesses the ambient space and does not appear in the line element. If one insists, it will end up to inconsistencies in the perturbed embedded space-time with gauge-fixing problems.

As it happens, the resulting perturbed geometry $g_{\mu\nu}$ can be bent and/or stretch without ripping the embedded space-time which it is not possible to do in the context of the Riemannian geometry as acknowledged by Riemann himself [84]. This feature is exclusive to dynamical embeddings. Due to the confinement, the standard cosmological theory cannot be applied beyond the embedded space-time. More specifically, it applies to the metric perturbation $\delta g_{\mu\nu}$ and to the induced equations onto the embedded space-time. Then, we calculate the linear perturbations for five-dimensions that the new geometry $\tilde{g}_{\mu\nu} = g_{\mu\nu}^{(0)} + \delta g_{\mu\nu}$ generated by Nash’s fluctuations is given by

$$\tilde{g}_{\mu\nu} = g_{\mu\nu}^{(0)} - 2\delta y k_{\mu\nu}^{(0)}, \quad (2.14)$$

and the related perturbed extrinsic curvature

$$\tilde{k}_{\mu\nu} = k_{\mu\nu}^{(0)} - 2\delta y^{(0)} g^{\sigma\rho} k_{\mu\sigma}^{(0)} k_{\nu\rho}^{(0)}, \quad (2.15)$$

where we can identify $\delta k_{\mu\nu} = -2\delta y^{(0)} g^{\sigma\rho} k_{\mu\sigma}^{(0)} k_{\nu\rho}^{(0)}$ valid in the ambient space. Using the Nash relation $\delta g_{\mu\nu} = -2k_{\mu\nu}^{(0)} \delta y$, δy is replaced and we obtain

$$\delta k_{\mu\nu} = {}^{(0)}g^{\sigma\rho} k_{\mu\sigma}^{(0)} \delta g_{\nu\rho} . \quad (2.16)$$

This is an important result since it correctly shows how the effects of the extrinsic quantities (e.g., δy and $\delta k_{\mu\nu}$) can be projected onto the perturbed four embedded space-time. In addition, by means of the induced field equations, as will be shown in the following, the resulting physics of the embedded space-time can be consistently studied.

2.2.2 Integrability conditions and induced equations

The integrability conditions of the embedding are given by the non-trivial components of the Riemann tensor of the embedding space as

$${}^5\mathcal{R}_{ABCD} \mathcal{Z}^A_{,\alpha} \mathcal{Z}^B_{,\beta} \mathcal{Z}^C_{,\gamma} \mathcal{Z}^D_{,\delta} = R_{\alpha\beta\gamma\delta} + (k_{\alpha\gamma} k_{\beta\delta} - k_{\alpha\delta} k_{\beta\gamma}) , \quad (2.17)$$

$${}^5\mathcal{R}_{ABCD} \mathcal{Z}^A_{,\alpha} \mathcal{Z}^B_{,\beta} \mathcal{Z}^C_{,\gamma} \eta^D = k_{\alpha[\beta;\gamma]} , \quad (2.18)$$

where ${}^5\mathcal{R}_{ABCD}$ is the five-dimensional Riemann tensor. The semicolon denotes covariant derivative with respect to the metric. The brackets apply the covariant derivatives to the adjoining indices only.

The first equation is called Gauss equation that shows that Riemann curvature of bulk space acts as a reference for the Riemann curvature of the embedded space-time. The second equation (Codazzi equation) evinces the projection of the Riemann tensor of the embedding space along the normal direction that is given by the tangent variation of the extrinsic curvature. This guarantees to reconstruct the five-dimensional geometry and to understand its properties from the dynamics of the four-dimensional space-time V_4 . These equations provide the necessary and sufficient conditions for the existence of the embedded manifold. As a solution of these equations, the analyticity of the embedding functions [85, 86] simplifies some results and imposes a maximum embedding dimension for all four-dimensional space-times to be $D = 10$. On the other hand, if one assumes that the deformed manifolds remain (at least) differentiable, the limit dimension for flat embeddings rises to $D = 14$ (such a number may be interesting for the study of super-algebras as in [87]), with a wide range of compatible signatures as shown by Greene [77] extending Nash theorem's results for a D -dimensional bulk $n(n+3)/2$, as n refers to the dimension of the embedded space. Also, $D = 14$ may induce a GUT based on a 45 parameter group like for example $SO(10)$ or equivalent, proposing that a larger gauge symmetry may be possible to obtain. Hence, the Nash theorem constitutes an important improvement over the traditional analytic embedding theorems [85, 86]. Thus, our present structure fulfills such requirement that limits the number of the extra-dimensions up to 10. Such limitation avoids bulk instabilities and the appearance of ghosts like those of some braneworld models. For instance, one of the points of Ref.[88] lies in the application of the longitudinal Goldstone mode acting as a brane bending mode. This was stated to keep fixed the induced metric on the brane. Unfortunately, this generates a classical instabilities (negative energy solutions) of this type of DGP model. In the realm of braneworlds program, it has been implemented mostly on particular models where the bulk has a fixed geometry and the space-time has a specific metric *ansatz*. Such new geometric quantity has a paramount role on the dynamics of the embedding itself. Then, the extrinsic curvature is not replaced by any additional principle or algebraic relation (e.g., Israel-Lanczos condition).

The “bending-stretching” (and eventually, the “ripping”) of the geometry is a natural effect of the extrinsic curvature once the embedding is properly defined.

It is important to point out that the confinement of the gauge fields to four dimensions is not really an assumption. It is a consequence of the fact that only in four dimensions the three-form resulting from the derivative of the Yang-Mills curvature tensor is isomorphic to the one-form current. Consequently, all known observable sources of gravitation composing the stress energy momentum tensor of the bulk T_{AB} are confined to these deformable four-dimensional space-times, independently of the value of the extra coordinate y . Unless experimental evidences prove the contrary, the confinement hypothesis imposes that the gauge interactions are only restricted to the embedded space-time, even through a mathematically constructed higher dimensional extensions of Yang-Mills equations are always possible in the context of strings and branes.

The induced field equations can be written by calculating the tangent e vector components of Eq. (2.2), in a five-dimensional bulk in the vicinity of V_4 such as

$$\mathcal{G}_{AB} = \begin{pmatrix} g_{\mu\nu}^{(0)} & 0 \\ 0 & 1 \end{pmatrix}. \quad (2.19)$$

Using Eq.(2.19), the induced background field equations are

$$G_{\mu\nu}^{(0)} + Q_{\mu\nu}^{(0)} = 8\pi G T_{\mu\nu}^{(0)}, \quad (2.20)$$

$$k_{\mu[\nu;\rho]}^{(0)} = 0, \quad (2.21)$$

where the energy-momentum tensor of the confined perfect fluid is denoted by $T_{\mu\nu}^{(0)}$ and G is the bare gravitational Newtonian constant. Here $G_{\mu\nu}^{(0)}$ denotes the four dimensional Einstein tensor and $Q_{\mu\nu}^{(0)}$ is called *deformation tensor*. The non-perturbed extrinsic term $Q_{\mu\nu}^{(0)}$ in Eq.(2.20) is given by

$$Q_{\mu\nu}^{(0)} = k_{\mu}^{(0)\rho} k_{\rho\nu}^{(0)} - k_{\mu\nu}^{(0)} h - \frac{1}{2} (K^2 - h^2) g_{\mu\nu}^{(0)}, \quad (2.22)$$

where we denote the mean curvature $h^2 = h \cdot h$ and $h = {}^0 g^{\mu\nu} {}^0 k_{\mu\nu}$. The term $K^2 = k^{\mu\nu(0)} k_{\mu\nu}^{(0)}$ is the Gaussian curvature. The equation (2.22) is readily conserved in the sense that

$$Q_{\mu\nu;\mu}^{(0)} = 0. \quad (2.23)$$

For a detail derivation of these equations, see Ref.[33] and references therein.

3 Background FLRW metric

Henceforth, after establishing the induced field equations, we can study the cosmological consequences in both background and perturbed universe. Firstly, we begin with the background cosmology. As it happens, the basic familiar line element of FLRW four-dimensional metric is given by

$$ds^2 = dt^2 - a^2 (dr^2 + r^2 d\theta^2 + r^2 \sin^2 \theta d\phi^2), \quad (3.1)$$

where the expansion factor is denoted by $a \equiv a(t)$. The coordinate t denotes the physical time. In the Newtonian frame, the former equations turns out to be

$$ds^2 = dt^2 - a^2 (dx^2 + dy^2 + dz^2). \quad (3.2)$$

3.1 Non perturbed field equation in an embedded space-time

By direct calculation of Eq.(3.2) in Eq.(2.20), the components of $G_{\mu\nu}^{(0)}$ are given as usual [89, 90]:

$$\begin{aligned} G_{ij}^{(0)} &= \frac{1}{a^2} \left(H^2 + 2\dot{H} \right) \delta_{ij} , \\ G_{4j}^{(0)} &= 0 , \\ G_{44}^{(0)} &= \frac{3}{a^2} H^2 , \end{aligned}$$

where the Hubble parameter is defined in the standard way by $H \equiv H(t) = \frac{\dot{a}}{a}$.

Since the extrinsic curvature is diagonal in FLRW space-time, one can find the components of extrinsic curvature using Eq.(2.21) that can be split into spatial and time parts:

$$k_{ij,k}^{(0)} - \Gamma_{ik}^a k_{aj}^{(0)} = k_{ik,j}^{(0)} - \Gamma_{ij}^a k_{ak}^{(0)} .$$

In the Newtonian frame, the spatial components are also symmetric and using the former relation one can obtain $k_{11}^{(0)} = k_{22}^{(0)} = k_{33}^{(0)} = b \equiv b(t)$, and straightforwardly

$$k_{ij}^{(0)} = \frac{b}{a^2} g_{ij}, \quad i, j = 1, 2, 3, \quad k_{44}^{(0)} = \frac{-1}{a} \frac{d}{dt} \frac{b}{a}, \quad (3.3)$$

and the following objects can be determined:

$$k_{44}^{(0)} = -\frac{b}{a^2} \left(\frac{B}{H} - 1 \right), \quad (3.4)$$

$$K^2 = \frac{b^2}{a^4} \left(\frac{B^2}{H^2} - 2\frac{B}{H} + 4 \right), \quad h = \frac{b}{a^2} \left(\frac{B}{H} + 2 \right), \quad (3.5)$$

$$Q_{ij}^{(0)} = -\frac{1}{3} Q_{44}^{(0)} \left(2\frac{B}{H} - 1 \right) \delta^{44} g_{ij}^{(0)}, \quad Q_{44}^{(0)} = -\frac{3b^2}{a^4}, \quad (3.6)$$

$$Q^{(0)} = -(K^2 - h^2) = \frac{6b^2}{a^4} \frac{B}{H}, \quad (3.7)$$

where we define the function $B = B(t) \equiv \frac{\dot{b}}{b}$ in analogy with the Hubble parameter. **We assume as a closure relation** $B/H = \text{const.} = \alpha_0$. Without any further ado, it can be easily solved by quadrature and gives the relation

$$b(t) = b_0 a(t)^{\alpha_0}. \quad (3.8)$$

It is worthy noting that the former relation completes univocally the set of the components of the extrinsic curvature in Eq.(3.3), as shown in previous works [33, 43].

3.2 Hydrodynamical equations

The stress energy tensor in a non-perturbed co-moving fluid is given by

$$T_{\mu\nu}^{(0)} = \left(\rho^{(0)} + p^{(0)} \right) u_\mu u_\nu - p^{(0)} g_{\mu\nu}^{(0)}; \quad u_\mu = \delta_\mu^4.$$

The conservation of $T_{\mu\nu;\mu}^{(0)} = 0$ leads to

$$\rho^{(0)} + 3H \left(\rho^{(0)} + p^{(0)} \right) = 0, \quad (3.9)$$

and the resulting Friedmann equation turns

$$H^2 = \frac{8}{3}\pi G\rho^{(0)} + \frac{b^2}{a^4}, \quad (3.10)$$

where $\rho^{(0)}$ is the present value of the non-perturbed matter density (hereon $\rho^{(0)} \equiv \rho_m^{(0)}(t)$). Thus, we write the matter density in terms of redshift as

$$\rho_m^{(0)}(t) = \rho_{m(0)}^{(0)}a^{-3} = \rho_{m(0)}^{(0)}(1+z)^3, \quad (3.11)$$

and we can rewrite Eq.(3.10) in terms of redshift as

$$H^2 = \frac{8}{3}\pi G\rho_{m(0)}^{(0)}(1+z)^3 + b_0^2(1+z)^{4-2\alpha_0}. \quad (3.12)$$

Using the definition of the cosmological parameter $\Omega_i = \frac{8\pi G}{3H_0^2}\rho_{i(0)}^{(0)}$, we finally have

$$\left(\frac{H}{H_0}\right)^2 = \Omega_{m(0)}(1+z)^3 + (1 - \Omega_{m(0)})(1+z)^{4-2\alpha_0}, \quad (3.13)$$

where $\Omega_{m(0)}$ is the current cosmological parameter for matter content and for a flat universe $\Omega_{ext(0)} = 1 - \Omega_{m(0)}$ and H_0 is the current value of Hubble constant in units of $\text{km.s}^{-1} \text{ Mpc}^{-1}$. It is worth noting that Eq.(3.13) with the α_0 -parameter nearly resembles the w CDM model in terms of comparison with their Friedmann equations at background level, where w is a dimensionless parameter of the fluid equation of state $w = \frac{p}{\rho}$ [91]. As we are going to show, the strikingly differences will appear at perturbation level. In this particular study, we do not consider the radiation term since it can be neglected for late times. Likewise, in conformal time η such that $dt = a(\eta)d\eta$ and $\mathcal{H} \equiv aH$, we can write the Friedmann equation in this frame as

$$\mathcal{H}^2 = \frac{k_0}{3}a^2 \left(\rho_m^{(0)}(t) + \frac{b_0^2}{k_0}a^{2\alpha_0-4} \right), \quad (3.14)$$

where $k_0 \equiv \frac{8}{3}\pi G$ and the conformal Hubble parameter is $\mathcal{H} = \frac{a'}{a}$. The prime symbol represents the conformal time derivative. Hence, the conformal time derivative of Hubble parameter is given by

$$\mathcal{H}' \equiv \frac{d\mathcal{H}}{d\eta} = -\frac{k_0}{6}a^2 \left(\rho_m^{(0)} + 3p^{(0)} + (\alpha_0 - 4)\frac{b_0^2}{k_0}a^{2\alpha_0-4} \right), \quad (3.15)$$

and completes the set of equations for a non-perturbed fluid in a conformal Newtonian gauge.

4 Transformations and gauge variables

Using the standard line element of FLRW metric in Euclidean coordinates in Eq.(3.2), one finds

$$ds^2 = a^2 (d\eta^2 - \delta_{ij}dx^i dx^j), \quad (4.1)$$

where $a = a(\eta)$ is the expansion parameter in conformal time. We start with the standard process as known in GR [89, 90, 92]. The novelty of this approach is the inclusion of the extrinsic curvature in the theoretical framework. Thus, let be the coordinate transformation $x^\alpha \rightarrow \tilde{x}^\alpha = x^\alpha + \xi^\alpha$ such as $\xi^\alpha \ll 1$, then we have for a second order tensor

$$\tilde{g}_{\alpha\beta}(\tilde{x}^\rho) = \frac{\partial x^\gamma}{\partial \tilde{x}^\alpha} \frac{\partial x^\delta}{\partial \tilde{x}^\beta} g_{\gamma\delta}(x^\rho).$$

Henceforth, we can write the perturbed metric tensor in the new coordinates $\delta\tilde{g}_{\alpha\beta}$ as

$$\delta\tilde{g}_{\alpha\beta} = \delta g_{\alpha\beta} - g_{\alpha\beta,\gamma}^{(0)}\xi^\gamma - g_{\alpha\delta}^{(0)}\xi_{,\beta}^\delta - g_{\beta\delta}^{(0)}\xi_{,\alpha}^\delta, \quad (4.2)$$

where the infinitesimally vector function $\xi^\alpha = \xi^{(4)} + \xi^i$ can be split into two parts

$$\xi^i = \xi^{i\perp} + \zeta^{,i},$$

in which $\xi^{i\perp}$ is the orthogonal part decomposition and ζ is a scalar function. The prime symbol denotes the derivative with respect to conformal time η . As a result, we can obtain

$$\delta\tilde{g}_{ij} = \delta g_{ij} + a^2 \left[2\frac{a'}{a}\delta_{ij}\xi^{(4)} + 2\zeta_{,ij} + \xi_{i,j}^\perp + \xi_{j,i}^\perp \right], \quad (4.3)$$

$$\delta\tilde{g}_{4i} = \delta g_{4i} + a^2 \left(\xi_{\perp i}' + \left[\zeta' - \xi^{(4)} \right]_{,i} \right), \quad (4.4)$$

$$\delta\tilde{g}_{44} = \delta g_{44} - 2a(a\xi^{(4)})'. \quad (4.5)$$

Using Eq.(4.2), we obtain a similar transformation for $k_{\mu\nu}$ as

$$\delta\tilde{k}_{\alpha\beta} = \delta k_{\alpha\beta} - k_{\alpha\beta,\gamma}^{(0)}\xi^\gamma - k_{\alpha\delta}^{(0)}\xi_{,\beta}^\delta - k_{\beta\delta}^{(0)}\xi_{,\alpha}^\delta. \quad (4.6)$$

And taking into account the Nash-Greene theorem

$$k_{\mu\nu}^{(0)} = -\frac{1}{2}g_{\mu\nu}^{\bullet(0)}, \quad (4.7)$$

where we denote $g_{\mu\nu}^{\bullet(0)} = \frac{\partial g_{\mu\nu}^{(0)}}{\partial y}$, and y is the coordinate of direction of perturbations from the background to the extra-dimensions (in this case, just one extra-dimension). Thus, we can rewrite Eq.(4.6) as

$$\delta\tilde{k}_{\alpha\beta} = \delta k_{\alpha\beta} + \frac{1}{2}g_{\alpha\beta,\gamma}^{\bullet(0)}\xi^\gamma + \frac{1}{2}g_{\alpha\delta}^{\bullet(0)}\xi_{,\beta}^\delta + \frac{1}{2}g_{\beta\delta}^{\bullet(0)}\xi_{,\alpha}^\delta, \quad (4.8)$$

and we get straightforwardly

$$\delta\tilde{k}_{ij} = \delta k_{ij} - (a^2)^\bullet \left[\frac{1}{2} \frac{((a^2)^\bullet)_{,4}}{(a^2)^\bullet} \delta_{ij}\xi^{(4)} + 2\zeta_{,ij} + \xi_{i,j}^\perp + \xi_{j,i}^\perp \right],$$

$$\delta\tilde{k}_{4i} = \delta k_{4i} + \frac{1}{2}(a^2)^\bullet \left(\xi_{\perp i}' + \left[\zeta' - \xi^{(4)} \right]_{,i} \right),$$

$$\delta\tilde{k}_{44} = \delta k_{44} + \left((a^2)^\bullet \xi^{(4)} \right)_{,4} - \frac{1}{2} \left((a^2)^\bullet \right)_{,4} \xi^{(4)}.$$

Taking the previous expressions and to avoid the implications of the ambiguity of two “times” coordinates, likewise the Rosen bi-metric theory [2, 93] that led to erroneous results such as a dipole gravitational waves, we adopt y as a set of space-like coordinates. Then, one obtains

$$\delta\tilde{k}_{ij} = \delta k_{ij}, \quad (4.9)$$

$$\delta\tilde{k}_{4i} = \delta k_{4i}, \quad (4.10)$$

$$\delta\tilde{k}_{44} = \delta k_{44}. \quad (4.11)$$

For scalar perturbations the metric takes the form

$$ds^2 = a^2[(1 + 2\phi)d\eta^2 + 2B_{,i}dx^i d\eta - ((1 - 2\psi)\delta_{ij} - 2E_{,ij})dx^i dx^j] , \quad (4.12)$$

where $\phi = \phi(\vec{x}, \eta)$, $\psi = \psi(\vec{x}, \eta)$, $B = B(\vec{x}, \eta)$ and $E = E(\vec{x}, \eta)$ are scalar functions.

For the tensors $G_{\mu\nu}$, $T_{\mu\nu}$ and $Q_{\mu\nu}$, one can use the same set of transformations. In this sense, for small perturbations, we can write the Einstein tensor in a coordinate system \tilde{x} as

$$\tilde{G}_{\mu\nu} = G_{\mu\nu}^{(0)} + \delta\tilde{G}_{\mu\nu} ,$$

where $\delta\tilde{G}_{\mu\nu}$ denotes linear perturbations in the new coordinate system

$$\delta\tilde{G}_{\alpha\beta} = \delta G_{\alpha\beta} - G_{\alpha\beta,\gamma}^{(0)}\xi^\gamma - G_{\alpha\delta}^{(0)}\xi_{,\beta}^\delta - G_{\beta\delta}^{(0)}\xi_{,\alpha}^\delta . \quad (4.13)$$

Immediately, we have a similar expression for $T_{\mu\nu}$

$$\tilde{T}_{\mu\nu} = T_{\mu\nu}^{(0)} + \delta\tilde{T}_{\mu\nu} ,$$

that leads to

$$\delta\tilde{T}_{\alpha\beta} = \delta T_{\alpha\beta} - T_{\alpha\beta,\gamma}^{(0)}\xi^\gamma - T_{\alpha\delta}^{(0)}\xi_{,\beta}^\delta - T_{\beta\delta}^{(0)}\xi_{,\alpha}^\delta , \quad (4.14)$$

and also, for the deformation tensor

$$\tilde{Q}_{\mu\nu} = Q_{\mu\nu}^{(0)} + \delta\tilde{Q}_{\mu\nu} ,$$

that leads to

$$\delta\tilde{Q}_{\alpha\beta} = \delta Q_{\alpha\beta} - Q_{\alpha\beta,\gamma}^{(0)}\xi^\gamma - Q_{\alpha\delta}^{(0)}\xi_{,\beta}^\delta - Q_{\beta\delta}^{(0)}\xi_{,\alpha}^\delta . \quad (4.15)$$

And using Eq.(4.12), we obtain for $\delta\tilde{G}_{\mu\nu}$:

$$\delta\tilde{G}_j{}^i = \delta G_j{}^i - ({}^{(0)}G_j{}^i)'(B - E') , \quad (4.16)$$

$$\delta\tilde{G}_i{}^4 = \delta G_i{}^4 - ({}^{(0)}G_4{}^4 - \frac{1}{3}({}^{(0)}G_k{}^k)(B - E')_{,i} , \quad (4.17)$$

$$\delta\tilde{G}_4{}^4 = \delta G_4{}^4 - ({}^{(0)}G_4{}^4)'(B - E') . \quad (4.18)$$

For the perturbed stress energy tensor $\delta\tilde{T}_{\mu\nu}$, one obtains the set of equations

$$\delta\tilde{T}_j{}^i = \delta T_j{}^i - ({}^{(0)}T_j{}^i)'(B - E') \quad (4.19)$$

$$\delta\tilde{T}_i{}^4 = \delta T_i{}^4 - ({}^{(0)}T_4{}^4 - \frac{1}{3}({}^{(0)}T_k{}^k)(B - E')_{,i} , \quad (4.20)$$

$$\delta\tilde{T}_4{}^4 = \delta T_4{}^4 - ({}^{(0)}T_4{}^4)'(B - E') . \quad (4.21)$$

Likewise, for the perturbed induced extrinsic part $\delta\tilde{Q}_{\mu\nu}$ we have

$$\delta\tilde{Q}_j{}^i = \delta Q_j{}^i - ({}^{(0)}Q_j{}^i)'(B - E') \quad (4.22)$$

$$\delta\tilde{Q}_i{}^4 = \delta Q_i{}^4 - ({}^{(0)}Q_4{}^4 - \frac{1}{3}({}^{(0)}Q_k{}^k)(B - E')_{,i} , \quad (4.23)$$

$$\delta\tilde{Q}_4{}^4 = \delta Q_4{}^4 - ({}^{(0)}Q_4{}^4)'(B - E') . \quad (4.24)$$

5 Scalar perturbations in Newtonian gauge

5.1 Perturbed gravitational equations

In longitudinal conformal Newtonian gauge, the main condition resides in the vanishing functions of $B = B(\vec{x}, \eta)$ and $E = E(\vec{x}, \eta)$, as well as the quantities $\xi^{(4)}, \xi', \zeta$. Hence, the metric in Eq.(4.12) turns to be

$$ds^2 = a^2[(1 + 2\Phi)d\eta^2 - (1 - 2\Psi)\delta_{ij}dx^i dx^j], \quad (5.1)$$

where $\Phi = \Phi(\vec{x}, \eta)$ and $\Psi = \Psi(\vec{x}, \eta)$ denote the Newtonian potential and the Newtonian curvature, respectively. In addition, we obtain a simplification of the previous transformations of the curvature-related quantities and the set of following outcomes:

$$\begin{aligned} \delta\tilde{g}_{44} &= \delta g_{44}; \quad \delta\tilde{g}_{4i} = \delta g_{4i} = 0; \quad \delta\tilde{g}_{ij} = \delta g_{ij}, \\ \delta\tilde{G}_4{}^4 &= \delta G_4{}^4; \quad \delta\tilde{G}_i{}^4 = \delta G_i{}^4; \quad \delta\tilde{G}_j{}^i = \delta G_j{}^i, \\ \delta\tilde{T}_4{}^4 &= \delta T_4{}^4; \quad \delta\tilde{T}_i{}^4 = \delta T_i{}^4; \quad \delta\tilde{T}_j{}^i = \delta T_j{}^i, \\ \delta\tilde{Q}_4{}^4 &= \delta Q_4{}^4; \quad \delta\tilde{Q}_i{}^4 = \delta Q_i{}^4; \quad \delta\tilde{Q}_j{}^i = \delta Q_j{}^i. \end{aligned} \quad (5.2)$$

Taking into account all the former results of Eqs.(5.2), we can write the perturbed induced field equations simply as

$$\delta G_\nu^\mu = 8\pi G \delta T_\nu^\mu - \delta Q_\nu^\mu, \quad (5.3)$$

$$\delta k_{\mu\nu;\rho} = \delta k_{\mu\rho;\nu}. \quad (5.4)$$

Using the Nash-Greene theorem, we notice that Codazzi equations in Eq.(5.4) do not propagate perturbations in which are confined to the background. In other words, Codazzi equations maintain their background form.

Applying Eq.(2.16) to Eq.(5.4), we obtain the background equation as in Eq.(2.21). In this sense, we have to look for the effects of the Nash-Greene fluctuations on the perturbed gravi-tensor equation and verify if the propagations of cosmological perturbations may occur. Thus, we can write the components of Eq.(5.3) as

$$\begin{aligned} \delta G_j^i &= 8\pi G \delta T_j^i - \delta Q_j^i, \\ \delta G_i^4 &= 8\pi G \delta T_i^4 - \delta Q_i^4, \\ \delta G_4^4 &= 8\pi G \delta T_4^4 - \delta Q_4^4, \end{aligned}$$

and using the conformal metric in Eq.(5.1), we have the components in the conformal Newtonian frame,

$$\mathcal{D}\delta_{ij} = \frac{1}{2}(\Psi - \Phi)_{,ij} + \frac{1}{2}a^2\delta Q_j^i - 4\pi G a^2 \delta T_j^i, \quad (5.5)$$

$$[\Psi' + \mathcal{H}\Phi]_{,i} = 4\pi G a^2 \delta T_i^4 - \frac{1}{2}a^2\delta Q_i^4, \quad (5.6)$$

$$\nabla^2\Psi - 3\mathcal{H}(\Psi' + \Phi\mathcal{H}) = 4\pi G a^2 \delta T_4^4 - \frac{1}{2}a^2\delta Q_4^4. \quad (5.7)$$

where $\mathcal{D} = [\Psi'' + \mathcal{H}(2\Psi + \Phi)' + (\mathcal{H}^2 + 2\mathcal{H}')\Phi + \frac{1}{2}\nabla^2(\Psi - \Phi)]$. Actually, the former resulting perturbed Einstein equations in conformal-Newtonian gauge coincide with those written in an

arbitrary coordinate system [92] which naturally relates this gauge to a gauge-invariant framework. As a result, the perturbations $\delta k_{\mu\nu}$ can be determined by the metric perturbations as shown in Eq.(2.16) in an adopted gauge. Moreover, the perturbation of the deformation tensor $Q_{\mu\nu}$ can be made from its background form in Eq.(2.22) and the resulting $k_{\mu\nu}$ perturbations from the Nash fluctuations of Eq.(2.16) such as

$$\delta Q_{\mu\nu} = -\frac{3}{2}(K^2 - h^2)\delta g_{\mu\nu} . \quad (5.8)$$

The quantity $\delta Q_{\mu\nu}$ is also independently conserved in a sense that $\delta Q_{\mu\nu;\nu} = 0$. Moreover, using the background relations of Eqs.(3.4), (3.5), (3.6), (3.7), we can determine the components of $\delta Q_{\mu\nu}$

$$\delta Q_j^i = 18\alpha_0 b_0^2 a^{2\alpha_0-2} \Psi \delta_j^i , \quad (5.9)$$

$$\delta Q_4^i = 0 , \quad (5.10)$$

$$\delta Q_4^4 = 18\alpha_0 b_0^2 a^{2\alpha_0-2} \Phi \delta_4^4 , \quad (5.11)$$

and we get the basic gauge invariant field equations modified by the extrinsic curvature in the conformal Newtonian gauge as

$$\mathcal{D}\delta_{ij} = 9\gamma_0 a^{2\alpha_0} \Psi \delta_{ij} + \frac{1}{2}(\Psi - \Phi)_{,ij} - 4\pi G a^2 \delta T_j^i , \quad (5.12)$$

$$[\Psi' + \mathcal{H}\Phi]_{,i} = 4\pi G a^2 \delta T_i^4 , \quad (5.13)$$

$$\nabla^2 \Psi - 3\mathcal{H}(\Psi' + \Phi\mathcal{H}) = 4\pi G a^2 \delta T_4^4 - 9\gamma_0 a^{2\alpha_0} \Phi , \quad (5.14)$$

where we denote $\gamma_0 = \alpha_0 b_0^2$.

5.2 Hydrodynamical gravitational perturbed equations

For a perturbed fluid with pressure p and density ρ , one can write the perturbed components of the related stress-tensor

$$\delta \tilde{T}_4^4 = \delta \rho , \quad (5.15)$$

$$\delta \tilde{T}_i^4 = \frac{1}{a}(\rho_0 + p_0)\delta u_{\parallel i} , \quad (5.16)$$

$$\delta \tilde{T}_j^i = -\delta p \delta_j^i , \quad (5.17)$$

where $\delta u_{\parallel i}$ denotes the tangent velocity potential and ρ_0 and p_0 denote the non-perturbed components of density and pressure, respectively. Hence, we can rewrite Eqs.(5.12), (5.13) and (5.14) as

$$\nabla^2 \Psi - 3\mathcal{H}(\Psi' + \Phi\mathcal{H}) = 4\pi G a^2 \delta \rho - 9\gamma_0 a^{2\alpha_0} \Phi , \quad (5.18)$$

$$[\Psi' + \mathcal{H}\Phi]_{,i} = 4\pi G a(\rho_0 + p_0)\delta u_{\parallel i} , \quad (5.19)$$

$$\mathcal{D}\delta_{ij} - \frac{1}{2}(\Psi - \Phi)_{,ij} = [4\pi G a^2 \delta p + 9\gamma_0 a^{2\alpha_0} \Psi] \delta_{ij} . \quad (5.20)$$

Those set of equations can be better understood in the Fourier k -space wave modes. Taking the Fourier transform of each main quantity (with subscript “ k ”), we obtain a new set of equations:

$$k^2 \Psi_k + 3\mathcal{H}(\Psi'_k + \Phi_k \mathcal{H}) = -4\pi G a^2 \delta \rho_k + 9\gamma_0 a^{2\alpha_0} \Phi_k , \quad (5.21)$$

$$\Psi'_k + \mathcal{H}\Phi_k = -4\pi G a^2 (\rho_0 + p_0) \theta , \quad (5.22)$$

where $\theta = ik^j \delta u_{\parallel j}$ denotes the divergence of fluid velocity in k -space. Finally, the third equation is given by

$$\mathcal{D}_k - \frac{1}{2} \hat{k}^i \cdot \hat{k}_i (\Psi_k - \Phi_k) = 4\pi G a^2 \delta p + 9\gamma_0 a^{2\alpha_0} \Psi_k , \quad (5.23)$$

where $\mathcal{D}_k = \Psi_k'' + \mathcal{H}(2\Psi_k + \Phi_k)' + (\mathcal{H}^2 + 2\mathcal{H}')\Phi_k + \frac{1}{2}k^2(\Psi_k - \Phi_k)$.

6 Matter density evolution under subhorizon regime

In order to obtain a bare response of an influence of the extrinsic terms, we do not consider anisotropic stresses and pressure for Eq.(5.22), Eq.(5.22) and Eq.(5.23), we obtain the following equation

$$k^2 \Phi_k + 3\mathcal{H} (\Phi_k' + \Phi_k \mathcal{H}) = -4\pi G a^2 \delta \rho_k + 9\gamma_0 a^{2\alpha_0} \Phi_k , \quad (6.1)$$

where the closure condition $\Psi = \Phi$ applies which is a result of the space-space traceless component from Eq.(5.20).

It is important to notice that when $\gamma_0 \rightarrow 0$ in Eq.(6.1), the standard GR equations are obtained and we can recover the subhorizon approximation with $k^2 \gg \mathcal{H}^2$ or $k^2 \gg a^2 H^2$ which means $\Phi_k'', \mathcal{H}\Phi_k' \sim 0$. To determine the gravitational potential Φ , we also need to work with the continuity and Euler equations from calculating the components $\delta T_{\mu;4}^\mu = 0$ and $\delta T_{\mu;i}^\mu = 0$ to obtain, respectively

$$\delta \rho' + (p_0 + \rho_0)(\nabla^2 u_i - 3\Phi') + 3\mathcal{H}(\delta p + \delta \rho) = 0, \quad (6.2)$$

$$\frac{d}{d\eta} [(p_0 + \rho_0)u_i] + (p_0 + \rho_0)(4\mathcal{H}u_i + \Phi) + \delta p = 0, \quad (6.3)$$

where the former expressions can be also written in terms of the fluid parameter w .

Taking Eq.(6.2) under a Fourier transform, we obtain the following equation in the k -space:

$$\delta \rho_k' - k^2 \rho_0 u_k - 3\rho_0 \Phi' + 3\mathcal{H} \delta \rho_k = 0 ,$$

which in subhorizon approximation gives

$$\delta \rho_k' - k^2 \rho_0 u_k \simeq 0 . \quad (6.4)$$

For the pressureless form of Eq.(6.3), we have

$$\rho_k' u_k + \rho_k u_k' + 4\mathcal{H} u_k \rho_k + \rho_k \Phi_k = 0 ,$$

and using the background formula from conservation equation of Eq.(3.9), we have

$$k^2 \rho_0 u_k' = -k^2 \mathcal{H} u_k - k^2 \Phi_k . \quad (6.5)$$

Performing the definition of the “contrast” matter density $\delta_m \equiv \frac{\delta \rho}{\rho_0}$, and using Eqs. (6.4), (6.5) and (6.1), we obtain a relation with Φ_k and δ_m as

$$k^2 \Phi_k = -4\pi G_{eff} a^2 \rho_0 \delta_m , \quad (6.6)$$

where G_{eff} is the effective Newtonian constant and is given by

$$G_{eff}(a, k) = \frac{G}{1 - \frac{9\gamma_0}{k^2} a^{2\alpha_0}}. \quad (6.7)$$

Taking the conformal time derivative of Eq.(6.4) and writing Eq.(6.5) in terms of δ_m and using Eq.(6.6), we obtain the equation of evolution of the contrast matter density $\delta_m(\eta)$ in conformal longitudinal Newtonian frame

$$\delta_m'' + \mathcal{H}\delta_m' - 4\pi G_{eff} a^2 \rho_0 \delta_m = 0. \quad (6.8)$$

To express Eq.(6.8) in terms of the physical time, we use the notation $\dot{\delta}_m \equiv \frac{\delta_m'}{a}$ and obtain the useful relation $\delta_m'' = a^2 \ddot{\delta}_m + a^2 H \dot{\delta}_m$. We are leading to

$$\ddot{\delta}_m(t) + 2H\dot{\delta}_m(t) - 4\pi G_{eff} \rho_0 \delta_m(t) = 0. \quad (6.9)$$

Thus, we obtain an alternatively way to express the former equation in terms of the expansion factor $a(t)$. We use the notation $\frac{d\delta_m(a)}{da} = \delta_m^\circ(a)$ and $\frac{d^2\delta_m(a)}{da^2} = \delta_m^{\circ\circ}(a)$, and obtain useful relations $\delta_m^\circ(a) = \frac{1}{a} \dot{\delta}_m(t)$ and $\delta_m^{\circ\circ}(a) = \frac{1}{a^2} \ddot{\delta}_m(t)$. Hence, the contrast matter density $\delta_m(a)$ is governed by the equation

$$\delta_m^{\circ\circ}(a) + \left(\frac{3}{a} + \frac{H^\circ(a)}{H(a)} \right) \delta_m^\circ(a) - \frac{3\Omega_{m0} G_{eff}/G}{2(H^2(a)/H_0^2)} \delta_m(a) = 0. \quad (6.10)$$

which solutions are possible only numerically. For instance, in the context of GR, where $G_{eff} = G$ that turns $\delta_m(a)$ independent of the scale k , with the fluid parameter w , one has the following solution

$$\delta(a) = a \cdot {}_2F_1 \left(-\frac{1}{3w}, \frac{1}{2} - \frac{1}{2w}; 1 - \frac{5}{6w}; a^{-3w}(1 - \Omega_m^{-1}) \right) \quad (6.11)$$

where ${}_2F_1(a, b; c; z)$ is a hypergeometric function.

7 Analysis on evolution of $f\sigma_8(z)$ and σ_8 -tensions

The form of the effective Newtonian constant is given by Eq.(6.7) as a result of the linear Nash-Greene fluctuations of the metric and the induced extrinsic curvature as shown in Eqs.(2.11) and (2.12). To alleviate the σ_8 -tension, a possible way is to modify gravity in some sense [25–31]. For the numerical implementation, we wrote a code using **Cobaya** [53, 54] sampler and the module **Classy** to include the cosmological theory code **CLASS** [94–96]. The joint analysis is made by using of data on the evolution of background parameter $H(z)$ and Ω_m distributions from SNIa Pantheon data [55], the clustering and weak lensing from DES Y1 [56], the BAO SDSS DR12 “consensus” galaxy sample [57] with redshift-space distortions (RSD) to compute growth data, $H(z)$ and BAO. The MCMC chains were analyzed by using **GetDist** [58] which was also used to make the contour plots. We sample the posterior distributions of the MCMC chains by means of Metropolis–Hastings algorithm [97, 98] in **Cobaya**. The runs were stopped by applying the Gelman-Rubin convergence criterion [99] that relies on $R - 1 < 0.01$. In the following, we summarize in Table (1) the mean marginalized posterior values for the parameters. We separated in four models. The first model refers to the “full” running on

Table 1. Marginalized constraints on the cosmological parameters using `GetDist`.

Parameters	model-1 (α_0)	model-2 ($\alpha_0 = 2$)	model-3 ($\alpha_0 = 1.5$)	model-4 ($\alpha_0 = 2.5$)
$H_0[km.s^{-1}.Mpc^{-1}]$	68.11 ± 1.780	67.941 ± 1.509	65.872 ± 0.704	66.964 ± 1.692
Ω_{m0}	0.312 ± 0.002	0.311 ± 0.065	0.306 ± 0.002	0.309 ± 0.003
σ_8	0.879 ± 0.058	0.820 ± 0.011	0.847 ± 0.026	0.864 ± 0.004
α_0	1.84 ± 0.773	2	1.5	2.5
χ^2 total	1123.86 ± 3.972	1123.55 ± 3.758	1121.8 ± 3.870	1122.34 ± 4.402

parameter space of α_0 and the model 2, α_0 is set to value 2 in order to mimic Λ CDM model, as Eq.(3.13) suggests. The same former idea was applied to defined the two other models for the values $\alpha_0 = 1.5$ (model 3) and $\alpha_0 = 2.5$ (model 4).

As Table (1) indicates, α_0 must sensitively deviate from the value 2 since the Λ CDM model can be mimicked with $\alpha_0 = 2$ (model 2) in order to not compromise the background evolution. As it happens, we analyse the situation when we extrapolate the parameters setting the model (3) and (4) with the values $\alpha_0 = (1.5, 2.5)$, respectively.

As a cosmography test, the evolution of the Hubble function is calculated using Eq.(3.13), and the deceleration parameter $q(z)$ is calculated by the standard form as

$$q(z) = \frac{1}{H(z)} \frac{dH(z)}{dz} (1+z) - 1. \quad (7.1)$$

Their profiles are shown in Figure (2) in terms of the redshift z .

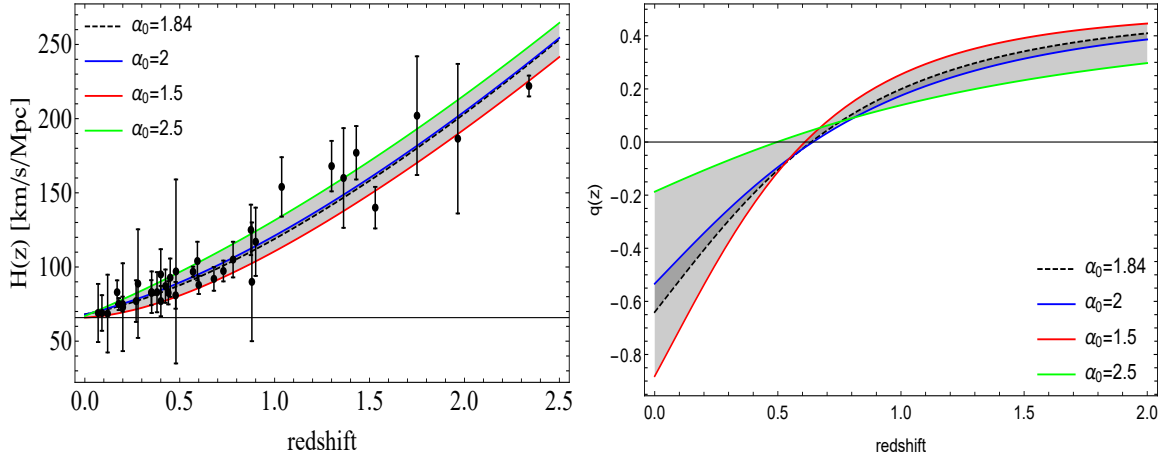


Figure 2. Hubble background evolution and deceleration parameter for the four models in terms of redshift. (For interpretation of the references to color in this figure legend, the reader is referred to the web version of this article.)

For the Hubble background evolution, we used datapoints from [55, 100] and some “clustering” measurements of $H(z)$ [101]. As a result, it is shown that α_0 is well constrained with values around 2, and all models respond well to Hubble evolution. A different situation occurs in the deceleration parameter $q(z)$ evolution. The model (1) ($\alpha_0 = 1.84$, dashed black line) and model (2) ($\alpha_0 = 2$, solid blue line) are compatible with the background evolution

in an acceleration regime, as expected. For the model (3) with $\alpha_0 = 1.5$, it induces a more negative deceleration parameter which leads to a negative fluid equation (in terms of a w fluid model) and values with $\alpha_0 < 1.5$ lead to an extreme negative fluid equation, which is ruled out by recent observations. The model (4) presents $\alpha_0 = 2.5$ with a “soft” deceleration value around $q_0 \sim -0.2$. For the values $\alpha_0 > 2.5$, the resulting background for these models is not compatible with the acceleration regime since $q > 0$ for any redshift and does not present a transition phase. Hence, the background stability is guaranteed in the range $\alpha_0 = [1.5, 2.5]$.

From Table (1), the marginalized values on the cosmological parameters were obtained from the MCMC chains. The 1 and 2 σ posteriors at 95% and 99% C.L. were computed with **GetDist** and are shown in the contour plots and PDFs in Figure (3) and (4). As a matter of comparison, we use the full chains of Planck2015 TT Low-TEB [11] and Planck2018 high- l temperature TTEE low- l low-E [12]³ to reproduce the contours in blue and red colors, respectively. In the plots, our model (model (1) with $\alpha_0 = 1.84$) is represented by the green color (the reader is referred to the web version of this article). As a result, we verified evidences for the alleviation on the tension particularly on σ_8 parameter and the drop-shaped contour includes at 1- σ level the Planck results in the $(\sigma_8 - H)$ plane and a reasonable congruence between the σ regions at 1- σ level in the $(\sigma_8 - \Omega_m)$ plane. Moreover, we mimic Λ CDM with $\alpha_0 = 2$ exhibiting the tensions of the contours between the parameters. In Figure (4), we present the contour plots for the models (2), (3) and (4) that show the tension of $(\sigma_8 - \Omega_m)$ plane and a considerable level of tension that persists in the $(\sigma_8 - H)$ and $(\Omega_m - H)$ planes, corroborating the tensions between the probes in model (2) and are aggravated in models (3) and (4) as shown in the related PDFs. For visualization purposes, we just compare the former models to the Planck2018 results.

Another test consist to analyse the evolution of the growth rate $f\sigma_8(a)$. A biased-free analysis may be performed by the measure of the quantity

$$f\sigma_8(a) \equiv f(a) \cdot \sigma_8(a) . \quad (7.2)$$

where $f(a) = \frac{\ln \delta}{\ln a}$ is the growth rate and the growth factor $\delta(a)$ is given by Eq.(6.10). In the χ^2 -statistics, one must consider the observed growth parameter $f(a_{obs})$ in minimization due to the Alcock-Paczynski effect to take into account redshift-space distortions. We use the “extended Gold-2018” growth-rate compilation as shown in Table 2 on the data points of SDSS [59–61], 6dFGS [62], IRAS [63, 64], 2MASS [63, 65], 2dFGRS [66], GAMA [67], BOSS [68], WiggleZ [69], Vipers [70], FastSound [71], BOSS Q [72] and an additional points from the 2018 SDSS-IV [27, 73–75]. These additional data points provide the growth-rate at relatively high redshifts. Moreover, as pointed out in Refs.[26, 27], to compatibilize the data dependence from the fiducial cosmology and another cosmological surveys, it is necessary to rescale the growth-rate data by the ratio $r(z)$ of the Hubble parameter $H(z)$ and the angular distance $D_A(z)$ by

$$r(z) = \frac{H(z)D_A(z)}{H_f(z)D_fA(z)} . \quad (7.3)$$

where the subscript “ f ” corresponds a quantity of fiducial cosmology. Similarly, the compatibilization of the related χ^2 statistics is also necessary. It can be done using the expression

$$\chi^2(\Omega_{0m}, \alpha_0, \sigma_8) = V^i C_{ij}^{-1} V_j , \quad (7.4)$$

³<https://pla.esac.esa.int/pla/#home>

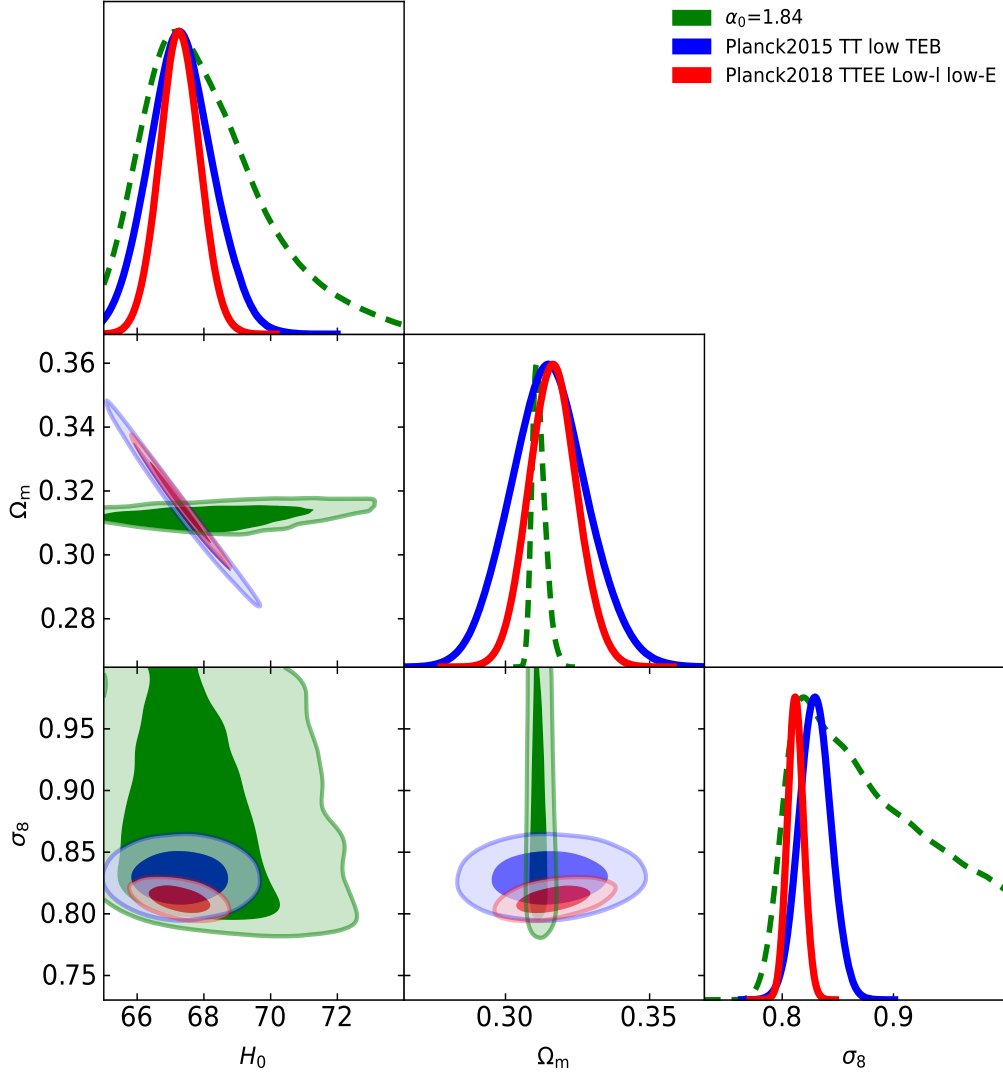


Figure 3. The contours with 95.4% and 99.7% C.L. of the marginalized cosmological parameter (H_0, Ω_m, σ_8). The panel shows an alleviation of the tension of the parameters. Blue contours indicate the chains from Planck 2015 CMB TT low TEB and the red contours refer to the Planck 2018 high- l temperature TTEE low- l low-E. The green contours refer to the resulted of the proposed model in this paper. (For interpretation of the references to color in this figure legend, the reader is referred to the web version of this article.)

where $V^i \equiv f\sigma_{8,i} - r(z_i)f\sigma_8(z_i, \Omega_{0m}, \alpha_0, \sigma_8)$ denotes a set of vectors that go up to i th-datapoints at redshift z_i for each $i = 1 \dots N$. N is the total number of datapoints of a related collection of a data. The set of $f\sigma_{8,i}$ datapoints come from theoretical predictions [26]. The set of C_{ij}^{-1} denotes the inverse covariance matrix. A final important correction concerns the necessity to disentangle the datapoints related to WiggleZ dark energy survey which are at first correlated. Then, the covariant matrix C_{ij} [69] is given by

$$C_{ij}^{wigglez} = 10^{-3} \begin{bmatrix} 6.400 & 2.570 & 0.000 \\ 2.570 & 3.969 & 2.540 \\ 0.000 & 2.540 & 5.184 \end{bmatrix} \quad (7.5)$$

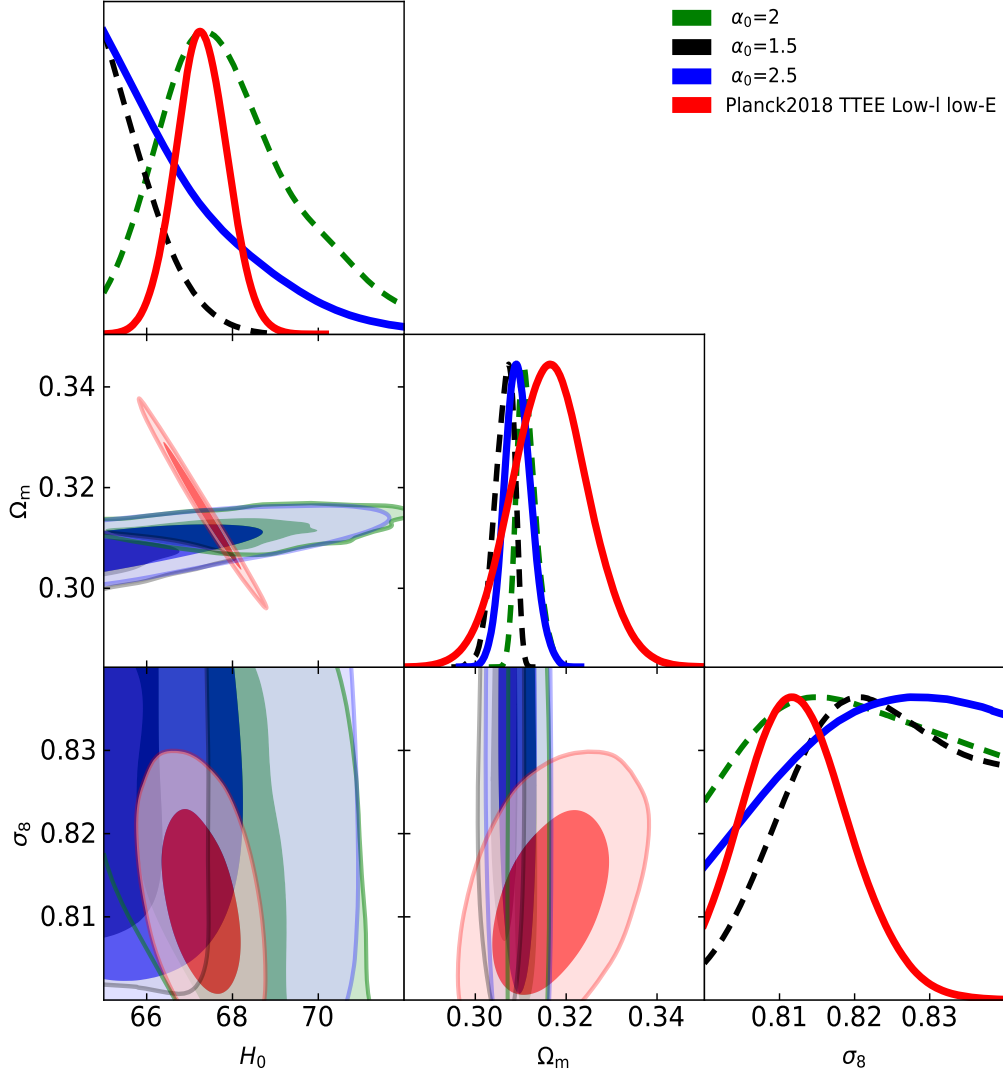


Figure 4. The contours with 95.4% and 99.7% C.L. of the marginalized cosmological parameter (H_0, Ω_m, σ_8). The panel shows the model-2 for $\alpha_0 = 2$ that reproduces the tensions of Planck/ Λ CDM cosmology which are aggravated in the model (3) ($\alpha_0 = 1.5$) and (4) ($\alpha_0 = 2.5$). The red contours refer to the Planck 2018 high- l temperature TTEE low- l low-E. The green contours refer to the result of the proposed model in this paper. (For interpretation of the references to color in this figure legend, the reader is referred to the web version of this article.)

and the resulting total matrix C_{ij}^{tot}

$$C_{ij}^{tot} = 10^{-3} \begin{bmatrix} \sigma_1^2 & 0 & 0 & \dots \\ 0 & C_{ij}^{wiggles} & 0 & \dots \\ 0 & 0 & \dots & \sigma_N^2 \end{bmatrix} \quad (7.6)$$

where the set of σ^2 's denote the N -variances.

In addition, we present in Figure (5) the resulting plot of the $f\sigma_8$ evolution from the datapoints of Table (2). As a result, the model (1) present a higher growth matter rate than model (2) (that mimics Λ CDM). On the other hand, extreme values for $f\sigma_8$ evolution are

Table 2. Datapoints the “extended Gold-2018” compilation of growth-rate [26] with additional points from BOSS Q [72] and SDSS-IV [27, 73–75].

Dataset	redshift	$f\sigma_8(z)$	Ω_m
6dFGS+SnIa	0.02	0.428 ± 0.0465	0.3
SnIa+IRAS	0.02	0.398 ± 0.065	0.3
2MASS	0.02	0.314 ± 0.048	0.266
SDSS-veloc	0.10	0.370 ± 0.130	0.3
SDSS-MGS	0.15	0.490 ± 0.145	0.31
2dFGRS	0.17	0.510 ± 0.060	0.3
GAMMA	0.18	0.360 ± 0.090	0.27
GAMMA	0.38	0.440 ± 0.090	0.27
SDSS-LRG-200	0.25	0.3512 ± 0.0583	0.25
SDSS-LRG-200	0.37	0.4602 ± 0.0378	0.25
BOSS-LOWZ	0.32	0.384 ± 0.095	0.274
SDSS-CMASS	0.59	0.488 ± 0.060	0.30711
WiggleZ	0.44	0.413 ± 0.080	0.27
WiggleZ	0.60	0.390 ± 0.063	0.27
WiggleZ	0.73	0.437 ± 0.072	0.27
Vipers PDR-2	0.60	0.550 ± 0.120	0.3
Vipers PDR-2	0.86	0.400 ± 0.110	0.3
FastSound	1.40	0.482 ± 0.116	0.270
BOSS-Q	1.52	0.426 ± 0.077	0.31
SDSS-IV	1.52	0.420 ± 0.076	0.26479
SDSS-IV	1.52	0.396 ± 0.079	0.31
SDSS-IV	0.978	0.379 ± 0.176	0.31
SDSS-IV	1.23	0.385 ± 0.099	0.31
SDSS-IV	1.526	0.342 ± 0.070	0.31
SDSS-IV	1.944	0.364 ± 0.106	0.31

found in models (3) and (4) that present the lower and the higher growth rates, respectively. This is compatible with our previous background results in Figure (2), since model (3) leads to a more intense accelerating mode with more negative values in $q(z)$ that avoids more the matter clustering. On the contrary, the “soft” acceleration of model (4) allows a more matter clustering profile and exhibits a higher growth matter rate as compared to the other models.

8 Remarks

In this paper we studied cosmic perturbations of matter in a search of understanding if the contribution of the extrinsic curvature to complement Einsteinian gravity is rather than semantics and relies on physical reality. It may pinpoint a renewed consideration of the concept of curvature, a paramount element of contemporary physics, as a fundamental physical agent itself. We work at two different (but correlated phases). First, we present the mathematical framework based on the embedding of Riemannian geometries in order to obtain the main expression of the embedded space-time deformations summarized in the extrinsic curvature perturbation $\delta k_{\mu\nu}$ and how its projection is possible onto the embedded space-time by means

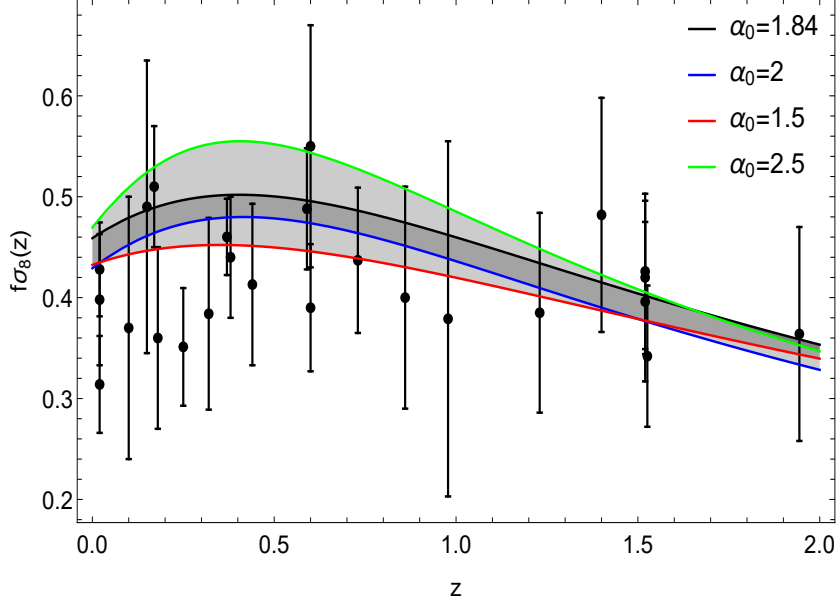


Figure 5. The growth rate $f\sigma_8(z)$ evolution for the four models in terms of redshift. (For interpretation of the references to color in this figure legend, the reader is referred to the web version of this article.)

of the Nash flow. We have shown that for dynamical embeddings, the perturbation coordinate y , that accesses the ambient space, does not appear in the four dimensional confined line element unlike that of rigid embedding model that need additional arguments to generate perturbations. Rather, the effects of the orthogonal perturbations of the background geometry are transferred by $\delta k_{\mu\nu}$ onto the perturbed embedded space-time. From the linear Nash-Greene perturbations of the metric, we have shown how to transpose the initial process in the background metric of the embedding of geometries to trigger the perturbations by the Lie transport. Secondly, in order to construct a viable physical model, we have focused on the embedded space-time with the obtainment of the induced field equations and on the related the perturbed field equations where the cosmological perturbation theory is applied. An interesting fact resides that in five dimensions the gravitational tensor equation is indeed a perturbed equation, once the perturbation of the Codazzi equation does not propagate cosmological perturbations being hampered by linear Nash's fluctuations. On the other hand, this landscape can be dramatically different in $dim \geq 6$ with appearance of new geometric objects, such as the third fundamental form $A_{\mu\nu a}$ that is associated to gauge fields. We also calculated the longitudinal Newtonian gauge of this framework in the simplest case that the gravitational potentials coincide $\Psi = \Phi$. Moreover, we have obtained in the subhorizon scale the contrast matter density ignited by the embedding equations. The finding of the matter overdensity equation δ_m is a paramount quantity for latter studies to identify any signature of modifications of gravity due to cosmic acceleration. We also have shown the determination of effective Newtonian constant G_{eff} . Furthermore, the σ tension paradigm may be solved as a result from a modification of gravity with a narrow set of values for the parameters from the joint analysis of SNIa Pantheon data, DES Y1 and the DR12 “consensus” galaxy sample marginalizing the parameters by means of **Cobaya** sampler and **GetDist** package. Our best results indicate the model with $\alpha_0 = 1.84$ and hence a consistent behaviour of $f\sigma_8$ growth descriptor. For completeness, we have established additional models. The model (2) mim-

ics Λ CDM with $\alpha_0 = 2$. Moreover, motivated by the structure of the Friedmann equation Eq.(3.13), we have applied a cosmography test on the models based on the evolution of $H(z)$ and the deceleration parameter $q(z)$ in order to evaluate their background stability which is obtained in the range $\alpha_0 = [1.5, 2.5]$. We also have shown that for the limiting models (3)($\alpha_0 = 1.5$) and (4)($\alpha_0 = 2.5$), they induce a more negative deceleration parameter (model (3)) or a “softer” acceleration (model (4)). Those profiles impact on the matter growth rate and out of the former α_0 range, the models have an unstable background and can be ruled out. These results pose an interesting scenario since the model seems to provide a necessary gravitational strength to correct the σ_8 tension. This was obtained by the inclusion of the extrinsic curvature as a pivot element to modify standard Einstein’s gravity. As prospects, the integrated Sachs–Wolfe (ISW) effect will be analysed in the light of larger surveys on dark energy and to study the impact of this model on CMB power spectrum.

9 Acknowledgements

The authors thank S. Nesseris for helpful insights on the `Mathematica` code and M.D. Maia for criticisms and suggestions. A. J. S. Capistrano thanks Fundação Araucária/PR for the Grant CP15/2017-P&D 67/2019.

References

- [1] V. Sahni, A. Starobinsky, Int. J. Mod. Phys. **D15**, 2105 (2006).
- [2] W. J. Percival et al., Mon. Not. Roy. Astron. Soc. **381**, 1053 (2007).
- [3] S. Alam et al. (BOSS), Mon. Not. Roy. Astron. Soc. **470**, 2617 (2017).
- [4] M. Kowalski et al. (Supernova Cosmology Project), Astrophys. J. **686**, 749 (2008).
- [5] A. H. Jaffe et al. (Boomerang), Phys. Rev. Lett. **86**, 3475 (2001).
- [6] L. Izzo, M. Muccino, E. Zaninoni, L. Amati, M. D. Valle, Astron. Astrophys. **582**, A115 (2015).
- [7] G. Efstathiou, P. Lemos, Mon. Not. Roy. Astron. Soc. **476**, 151 (2017).
- [8] S. W. Allen, D. A. Rapetti, R. W. Schmidt, H. Ebeling, R. G. Morris, A. C. Fabian, Mon. Not. Roy. Astron. Soc. **383**, 879 (2008).
- [9] E. Baxter et al., Mon. Not. Roy. Astron. Soc. **461**, 4099 (2016).
- [10] R. Chávez, et al. Mon. Not. Roy. Astron. Soc. **462**, 2431 (2016).
- [11] N. Aghanim et al., (Planck Collaboration) A&A 594, A11 (2016).
- [12] N. Aghanim et al., (Planck Collaboration), A&A 641, A5 (2020).
- [13] R. J. Nemiroff, R. Joshi, B. R. Atla, J. Cosmol. Astropart. Phys. **006**, (2016).
- [14] B. Santos, A. A. Coley, N. Chandrachani Devi, J. S. Alcaniz, J. Cosmol. Astropart. Phys. **002**, 047 (2017).
- [15] P. Kumar, C. P. Singh, Astrophys Space Sci. **362**, 52 (2017).
- [16] H. E. S. Velten, R.F. vom Marttens, W. Zimdahl, Eur.Phys.J. **C74**, 11, 3160 (2014).
- [17] J. Sultana, Mon. Not. Roy. Astron. Soc. **457**(1), 212 (2016).
- [18] N. Sivanandam, Phys. Rev. D **87**, 083514 (2013).
- [19] K. Nozari, N. Behrouz, N. Rashidi, Adv. High En. Phys. **5697022014**, (2014).

- [20] X. Fan, N. A. Bahcall, R. Cen., *Astrophys. J. Lett.* **490**, 123 (1997).
- [21] G. E. Addison, et al. *Astrophys. J.* **853**, 2, 119 (2018).
- [22] R. A. Battye, T. Charnock, A. Moss, *Phys. Rev.* **D91**, 10, 103508 (2015).
- [23] S. Birrer et al., *Mon. Not. Roy. Astron. Soc.* **484**, 4726 (2019).
- [24] I. G. McCarthy, S. Bird, J. Schaye, J. Harnois-Deraps, A. S. Font, L. Van Waerbeke, *Mon. Not. Roy. Astron. Soc.* **476**, 3, 2999 (2018).
- [25] Eva-Maria Mueller et al., *Mon. Not. Roy. Astron. Soc.* **475**, 2, 2122 (2018).
- [26] S. Nesseris, G. Pantazis, L. Perivolaropoulos, *Phys. Rev. D* **96**, 2, 023542 (2017).
- [27] L. Kazantzidis, L. Perivolaropoulos, *Phys. Rev. D* **97**, 103503 (2018).
- [28] R. Gannouji, L. Kazantzidis, L. Perivolaropoulos, D. Polarski, *Phys. Rev. D* **98**, 104044 (2018).
- [29] E. Di Valentino, E. Linder, A. Melchiorri, *Phys. Rev. D* **97**, 043528 (2018).
- [30] G. Lambiase, S. Mohanty, A. Narang, P. Parashari, *Eur. Phys. J. C* **79**, 14 (2019).
- [31] S. Bahamonde, K. F. Dialektopoulos, J. L. Said, *Phys. Rev. D* **100**, 064018 (2019).
- [32] M. D. Maia, E. M. Monte, *Phys. Lett. A* **297**, 2, 9 (2002).
- [33] M. D. Maia, E. M. Monte, J. M. F. Maia, J. S. Alcaniz, *Class.Quantum Grav.* **22**, 1623 (2005).
- [34] M. D. Maia, N. Silva, M. C. B. Fernandes, *Journ. High En.Phys.* **04**, 047 (2007).
- [35] N. Arkani-Hamed et al, *Phys. Lett. B* **429**, 263 (1998).
- [36] L. Randall, R. Sundrum, *Phys. Rev. Lett.* **83**, 3370 (1999).
- [37] L. Randall, R. Sundrum, *Phys. Rev. Lett.* **83**, 4690 (1999).
- [38] G. Dvali, G. Gabadadze, M. Porrati, *Phys. Lett.B* **485**, 1-3, 208 (2000).
- [39] R. A. Battyea, B. Carter, *Phys. Lett. B* **509**, 331 (2001).
- [40] M. Heydari-Farda, H. R. Sepangi, *Phys.Lett. B* **649**, 1 (2007).
- [41] S. Jalalzadeh, M. Mehrnia, H. R. Sepangi, *Class.Quant.Grav.* **26**, 155007 (2009).
- [42] M. D. Maia, *Geometry of the fundamental interactions*, Springer: New York, p.166 (2011).
- [43] M. D. Maia, A. J. S Capistrano, J. S. Alcaniz, E. M. Monte, *Gen. Rel. Grav.* **10**, 2685 (2011).
- [44] A. Ranjbar, H. R. Sepangi, S. Shahidi, *Ann. Phys.* **327**, 3170 (2012).
- [45] A. J. S. Capistrano, L. A. Cabral, *Ann. Phys.* **384**, 64 (2014).
- [46] S. Jalalzadeh, T. Rostami, *Int. Journ. Mod. Phys. D* **24**, 4, 1550027 (2015).
- [47] A. J. S. Capistrano, *Mon. Not. Roy. Astron.Soc.* **448**, 1232 (2015).
- [48] A. J. S. Capistrano, L. A. Cabral, *Phys. Scr.* **91**, 105001 (2016).
- [49] A. J. S. Capistrano, L. A. Cabral, *Class. Quantum Grav.* **33**, 245006 (2016).
- [50] A. J. S. Capistrano, A. C. Gutiérrez-Piñeres, S. C. Ulhoa, R. G. G. Amorim, *Ann. Phys.* **380**, 106 (2017).
- [51] A. J. S. Capistrano, *Ann. Phys. (Berlin)*, 1700232 (2017).
- [52] A.J. S. Capistrano, *Phys. Rev. D* **100**, 064049-1 (2019).
- [53] J. Torrado, A. Lewis, *Cobaya: Code for Bayesian Analysis of hierarchical physical models*, arXiv:2005.05290[astro-ph.IM].
- [54] J. Torrado, A. Lewis, *Cobaya: Bayesian analysis in cosmology*, [ascl:1910.019].
- [55] D. M. Scolnic et al. 2018 *ApJ* 859 101.

- [56] T. M. C. Abbott (DES collaboration), Phys. Rev. D **98**, 043526 (2018).
- [57] S. Alam et al, Mon. Not. Roy. Astron. Soc. **470**, 3, 2617 (2017).
- [58] A. Lewis, *GetDist: a Python package for analysing Monte Carlo samples*, arXiv:1910.13970[astro-ph.IM].
- [59] L. Samushia, W. J. Percival, A. Raccañelli, Mon. Not. Roy. Astron. Soc. **420**, 2102 (2012).
- [60] C. Howlett, A. Ross, L. Samushia, W. Percival, M. Manera, Mon. Not. Roy. Astron. Soc. **449**, 1, 848 (2015).
- [61] M. Feix, A. Nusser, E. Branchini, Phys. Rev. Lett. **115**, 1, 011301 (2015).
- [62] D. Huterer, D. Shafer, D. Scolnic and F. Schmidt, J. Cosmol. Astropart. Phys. **05**, 015, 1705 (2017).
- [63] M. J. Hudson, S. J. Turnbull, Astrophys. J. **751**, L30 (2013).
- [64] S. J. Turnbull, et al., Mon. Not. Roy. Astron. Soc. **420**, 447, (2012).
- [65] M. Davis et al., Mon. Not. Roy. Astron. Soc. **413**, 2906, (2011).
- [66] Y. S. Song, W. J. Percival, J. Cosmol. Astropart. Phys. **0910**, 004 (2009).
- [67] C. Blake et al., Mon. Not. Roy. Astron. Soc. **436**, 3089 (2013).
- [68] A. G. Sanchez et al., Mon. Not. Roy. Astron. Soc. **440**, 3, 2692 (2014).
- [69] C. Blake et al., Mon. Not. Roy. Astron. Soc. **425**, 405 (2012).
- [70] A. Pezzotta et al., Astron. Astrophys. **604**, A33 (2017).
- [71] T. Okumura et al., Publ. Astron. Soc. Jap. **68**, 3, 38 (2016).
- [72] P. Zarrouk et al., Mon. Not. Roy. Astron. Soc. **477**, 2, 1639, (2018).
- [73] Héctor Gil-Marín et al., Monthly Not. R. Astron. Soc. **477**, 2, 1604-1638 (2018).
- [74] J. Hou et al., Mon. Not. Roy. Astron. Soc. **480**, 2, 2521-2534 (2018).
- [75] Gong-Bo Zhao et al., Mon. Not. Roy. Astron. Soc. **482**, 3, 3497-3513 (2019).
- [76] J. Nash, Ann. Maths. **63**, 20 (1956).
- [77] R. Greene, Memoirs Amer. Math. Soc. **97**, (1970).
- [78] S. K. Donaldson, Contemporary Mathematics (AMS) **35**, 201 (1984).
- [79] C. H. Taubes, Contemporary Mathematics (AMS) **35**, 493 (1984).
- [80] C. S. Lim, Prog. Theor. Exp. Phys., 02A101 (2014).
- [81] J. Rosen, Rev. Mod. Phys. **37**, 204 (1965).
- [82] L. P. Eisenhart, Non-Riemannian geometry, Dover, New York: NY, (2005).
- [83] Y. Choquet-Bruhat, J. Jr York, Mathematics of Gravitation, Warsaw: Institute of Mathematics, Polish Academy of Sciences, (1997).
- [84] B. Riemann (Translated by W. K. Clifford), Nature **8**, 114 and 136 (1873).
- [85] M. Janet, Ann. Soc. Pol. Mat 5, (1928).
- [86] E. Cartan Ann. Soc. Pol. Mat 6, 1 (1927).
- [87] I. Bars, Phys. Lett. B **403**, 257, (1997).
- [88] M. A. Luty, M. Porrati, R. Rattazzi, JHEP 0309, 029 (2003).
- [89] H. Kodama, M. Sasaki, Cosmological perturbation theory, Prog. Theor. Phys. **78**, (1984).
- [90] V. Mukhanov, Physical foundations of Cosmology, Cambridge University Press: UK, (2005).

- [91] M. S. Turner, M. White, Phys. Rev. D **56**, 4439 (1987).
- [92] V.F. Mukhanov, H.A. Feldman, R.H. Brandenberger, Physics Reports 215, 5-6, 203—333 (1992).
- [93] N. Rosen, Gen. Rev. Grav. **4435** (1973).
- [94] J. Lesgourgues, *CLASS I: Overview*, arXiv:1104.2932 [astro-ph.IM]
- [95] D. Blas, J. Lesgourgues, T. Tram, JCAP 07, 034, (2011).
- [96] E. Di Dio, F. Montanari, J. Lesgourgues, R. Durrer, JCAP 11, 044, (2013).
- [97] A. Lewis, S. Bridle, Phys.Rev.D 66, 103511 (2002).
- [98] A. Lewis, Phys.Rev.D 87, 103529 (2013).
- [99] A. Gelman, D. Rubin, Statistical Science 7, 457 (1992).
- [100] M. Moresco et al., JCAP 1208, 006 (2012).
- [101] Rui-Yun Guo, X. Zhang, Eur. Phys. J. C 76, 163, (2016).